Supporting Information

J-aggregation induced NIR-II fluorescence: an aza-BODIPY luminogen for efficient phototheranostics

Na Yang,[ab] Shuang Song,[b] Mahmood Hassan Akhtar,[b] Chang Liu,[ab] Lang Yao,[ab] Jiayuan Yu, [b] Ying Li,[b] Qianxue Li,[c] Di He*[b], and Cong Yu*[ab]

a. School of Applied Chemistry and Engineering, University of Science and Technology of China, Hefei 230026, P.R. China.

b. State Key Laboratory of Electroanalytical Chemistry, Changchun Institute of Applied Chemistry, Chinese Academy of Sciences, Changchun 130022, P.R. China.

c. Changchun Veterinary Research Institute, Chinese Academy of Agricultural Sciences, Changchun 130122, P.R. China.

Experimental section

Chemicals and Materials

All chemical reagents were purchased from Aladdin or Energy Chemical Co., Ltd. Commercially available reagents were analytical reagent grade and used directly without further purification. DSPEG-PEG2000-NH_2 was purchased from Chongqing Yusi medical technology cable Co., Ltd. Indocyanine green (ICG) was purchased from Bide Medicine Co., Ltd. DMEM medium were purchased from HyClone Life Technologies. Phosphate buffered saline (PBS), fetal bovine serum (FBS), 0.25% Trypsin-EDTA, Cell Counting Kit-8 (CCK-8) and penicillin/streptomycin (P/S) were purchased from BBI Life Technologies. Rat LLC cell lines were obtained from Procell

Life Science &Technology Co., Ltd. Millipore deionized (DI) water (18.2 MΩ cm^{-1}, 25 °C) was used to prepare all assay solutions.

Apparatus and Characterization

^{1}H and ^{13}C NMR spectra were recorded on a Bruker Avance III 500/400 MHz spectrometer using residual proton or carbon signal of the deuterated solvent as internal standard. Mass spectra were recorded on a Bruker Mass spectrometer (Bruker Daltonic flex analysis). Chemical shifts are reported in parts per million. H-600 electron microscope (TEM, Hitachi, Japan) was used to characterize the morphology of the TAJ nanoparticles. Cary 50 Bio Spectrophotometer (Varian Inc., CA, USA) was used to record the UV–vis absorption spectra using a 1 cm cuvette. Fluorescence emission spectra were recorded using a FluoroLog-3 spectrofluorometer (Horiba Inc., USA) at an ambient temperature. Cell viability data were recorded by a Synergy microplate reader (BioTek, USA).

Synthesis and characterization of T-1

1.77 g 4-diethylaminobenzaldehyde and 1.26 g 3-acetylthiophene were mixed in 100 mL EtOH, and then NaOH solution (2.5 M, 30 mL) was added. The reaction solution was stirred at room temperature for 24 h, a yellow solid was filtered and dried without further purification. ^{1}H NMR (400 MHz, DMSO-d_6) δ (ppm): 8.20 (dd, J = 3.8, 1.1 Hz, 1H), 7.97 (dd, J = 5.0, 1.1 Hz, 1H), 7.72-7.58 (m, 3H), 7.54-7.50 (m, 1H), 7.28 (dd, J = 5.0, 3.8 Hz, 1H), 6.80-6.61 (m, 2H), 3.42 (q, J = 7.0 Hz, 4H), 1.13 (t, J = 7.0 Hz, 6H).

Synthesis and characterization of T-2

1.42 g compound T-1 was dissolved in a mixture of methanol (10 mL), diethylamine (7.5 mL) and nitromethane (4 mL), and the reaction mixture was refluxed overnight. After cooling to room temperature, 1 M HCl was used to neutralize the solution, and the crude product was extracted with CH_2Cl_2 (3×50 mL). Na_2SO_4 was used to dry the combined organics. Solvent was cleaned up under reduced pressure. The final product was acquired by chromatography (petroleum ether/EtOAc, 9:1). ^{1}H NMR (500 MHz, $CDCl_3$) δ (ppm): 7.69 (dd, *J* = 3.8, 1.1 Hz, 1H), 7.64 (dd, *J* = 3.8, 1.1 Hz, 1H), 7.13-7.06 (m, 3H), 6.60 (d, *J* = 8.4 Hz, 2H), 4.80-4.76 (m, 1H), 4.66-4.62 (m, 1H), 4.08-4.06 (m, 1H), 3.35-3.29 (m, 6H), 1.13 (t, *J* = 7.0 Hz, 6H).

Synthesis and characterization of T-3

0.22 g compound T-2 and 1.40 g ammonium acetate were mixed in 8 mL n-butanol, then reacted at 110 ºC for 16 h. After solvent was removed, the residue was filtered and washed with cool ethanol three times. Compound T-3 of blue color was used directly without further purification.

Synthesis and characterization of TA

0.11 g compound T-3 was dissolved in a mixture of dry CH_2Cl_2 (5 mL), DIEA (1 mL) and BF3•OEt_2 (0.8 mL). The solution was reacted at room temperature for 12 h. The final product TA as blue solid was acquired by chromatography (petroleum

ether/EtOAc, 8:1). ^{1}H NMR (500 MHz, DMSO-d_6) δ (ppm) 8.19 (dd, J = 3.8, 1.1 Hz, 2H), 8.13-8.11 (m, 4H), 7.98 (dd, J = 3.8, 1.1 Hz, 2H), 7.35-7.32 (m,4H), 6.83-6.81(m, 4H), 3.49 (q, J = 7.0 Hz, 8H), 1.18 (t, J = 7.0 Hz, 12H). ^{13}C NMR (101 MHz, $CDCl_3$) (ppm): 148.48, 142.56, 134.83, 131.74, 131.18, 129.69, 129.94, 129.42, 120.24, 114.23, 111.33, 44.64, 12.73; HR-MS (m/z, ESI): calculated for $C_{36}H_{36}BF_2N_5S_2$ $[M]^+$ 651.2473, found 652.2528, $[M+H]^+$.

Preparation and characterization of dye-assemblies

Typically, a THF solution of TA was added deionized water and waggled rapidly about 30 s. After standing for 30 minutes, the samples were used for further testing.

Absorption and emission spectra: TA (20 μM) in THF/H_2O mixture (water fractions was 80%) was prepared. 1% Triton X-100 was used to disrupt the aggregation of TA.

TEM: The sample was prepared by TA (40 μM) in THF/H_2O mixture (water fractions was 80%). Then, TEM was used to observe the morphology of aggregates.

Preparation of the TAJ nanoparticles

THF solution (1 mL) containing DSPE-PEG2000-NH_2 (10 mg) and TA (1 mg) were added dropwise into an aqueous solution (6 mL), and the mixture was stirred for 0.5 h at ambient temperature. The solution was then dialyzed against ultrapure water for 24 h in an 8000 molecular weight dialysis bag. The aqueous solution was further centrifuged with a centrifugal-filter (MWCO = 10 kDa) at 6000 rpm for 10 min and filtered through a 0.22 μm filter for further experiments.

Photothermal effect of TAJ NPs

First of all, in order to evaluate the effect of power density on photothermal behavior of nanoparticles, TAJ NPs (10 μM) were irradiated by 808 nm laser at different power densities (0.5, 1, 1.25, 1.5, 2.0 W/cm^2). The temperature changes were monitored by a thermometer. Then, the effect of concentration on temperature was studied. Pure water and different concentration of TAJ NPs (10, 20, 30, 40 μM) were prepared and irradiated by 808 nm laser with a power density of 1.25 W/cm^2 for 10 min.

To measure the photothermal conversion efficiency, TAJ-NPs (30 μM) were exposed to 808 nm irradiation at 1.25 W/cm^2 for 10 min, and then the solution was cooled down to room temperature. The temperature of the solution was recorded at an interval of 10 s during this process. The photothermal conversion efficiency (η) was measured according to the reported method.

$$\eta = \frac{hS(T_{max} - T_{amb}) - Q_{Dis}}{I(1 - 10^{-A_{808}})}$$

$$hs = \frac{mC_{water}}{\tau_s}$$

$$\theta = \frac{T - T_{amb}}{T_{max} - T_{amb}} \quad t = -\tau_s In(\theta)$$

where h is the heat transfer coefficient, S is the surface area of the container. T_{max} is the maximum steady-state temperature of the TAJ NPs containing aqueous solution, T_{amb} is the environmental temperature. I is the laser power density, A_{808} is the absorbance of the TAJ NPs at 808 nm and Q_{Dis} is the heat associated with light absorption by the solvent. The variable τ_s is the sample-system time constant, and C_{water} are the mass and

heat capacity (4.2×10^3 J/kg ºC) of deionized water.

Besides, the photothermal stability of TAJ NPs (30 μM) was measured by five cycles of heating-cooling processes (808 nm, 1.25 W/cm^2).

Fluorescence quantum yield (QY) measurement

The QY of the NPs was determined as follows, using Flav7 as the reference (QY = 0.53%). Flav7 was diluted with 1,2-dichloroethane to a series of samples. Then the emission spectra were integrated into the 1000 to 1500 nm region. The same procedures were performed for the samples in PBS buffer. The obtained emission integration was plotted against the absorption intensity and fitted into a linear relationship. The QY calculation Equation was as follows:

$$\Phi = \varphi_{ref} \times (n^2_{sample}/n^2_{ref}) (S_{sample}/S_{ref})$$

where Φ is the QY of the TAJ NPs, φ_{ref} is the QY of Flav7, S_{sample} and S_{ref} are the slopes obtained by linear fitting of the integrated emission spectra of the TAJ NPs and Flav7 against the absorbance at 808 nm, and n_{sample} and n_{ref} are the refractive indices of H_2O and dichloroethane, respectively.

Hemolysis Test

Firstly, about 0.5 mL of peripheral blood was taken from the venous plexus around the eyes of Balb/c mice. The blood was then centrifuged at 3000 rpm for 15 min to separate the plasma and red blood cells, and the above steps were repeated thrice to ensure that

the plasma was completely washed away to obtain red blood cells. The red blood cells were dispersed in PBS to obtain a red blood cell dispersion with a concentration of 2%. Next, 100 μL red blood cell dispersions were mixed with equal volumes of TAJ NPs at different concentrations and incubated in a shaker at 37°C for 1 h. Finally, the mixed solution was centrifuged again at 3000 rpm for 15 min, and the changes in the supernatant were observed. Meanwhile, the supernatant was taken and the red blood cell absorption at 545 nm was detected by a microplate reader to evaluate the hemolysis of TAJ NPs.

Cell culture

LLC cells were cultured in DMEM culture medium containing 10% fetal bovine serum and 1% antibiotics penicillin/streptomycin (100 U/mL) at 37 ºC, 5% CO_2.

Cytotoxicity

Cytotoxicity of the TAJ NPs was evaluated by the traditional CCK-8 assay. 5×10^3 cells were seeded in a 96-well plate and grown overnight in an incubator. Various amounts of TAJ NPs were added respectively and the samples were incubated for an additional 24 h. The culture medium was removed and 200 μL of fresh culture medium was added. One set of the cell samples was irradiated with light for 10 min (808 nm, 1.25 W/cm^2). Another set was not irradiated. Then, the culture medium was removed and 200 μL of fresh culture medium (containing 10% CCK-8) was added. The cells were further incubated for 2 h, and the absorption values at 450 nm were recorded by a

microplate reader.

Animal experiments

All animal experiments in this work were handled under protocols approved by the Institutional Animal Care and Use Committee of Changchun Institute of Applied Chemistry, Chinese Academy of Sciences (Protocol number: 2022001128). Female C57 mice (6-8 weeks old) were obtained from Liaoning Changsheng Biotechnology Co., Ltd. The tumor-bearing models were established by inoculating murine LLC cancer cells (100 μL, 4×10^5 cells/mL in PBS) subcutaneously in C57 mice. The mice were further treated when the volume of the tumor reaches about 120 mm^3.

***In vivo* NIR-II fluorescence imaging**

All mice were shaved using hair removal cream and anesthetized with isoflurane before the experiment, and then placed on the imaging table. 3 mice were used as parallel controls in each imaging experiment. All NIR-II images were collected on a two-dimensional InGaAs array (Rappter-640) with a laser of 808 nm and a power density of 65 mW/cm^2. Images were collected using different long-pass filters. Meanwhile, except for blood vascular imaging using Balb/c mice, the rest images without special notice were all using C57 mice. Three mice were selected to perform the NIR-II fluorescence imaging. The mice were intravenously injected with the TAJ NPs (1 mM, 100 μL) and the fluorescence microscopy images were captured at different time intervals. After 36 h, the mice were sacrificed and fluorescence images of tumor, heart,

liver, lung, kidney and spleen were recorded.

In vivo photothermal therapy

15 tumor-bearing mice were divided randomly in three groups on average, as bellow (i) Group 1 “PBS+laser”; (ii) Group 2 “TAJ NPs” and (iii) Group 3 “TAJ NPs+laser”. Mice were injected on the first day of treatment. The experimental group mice were injected with TAJ NPs (100 μL, 300 μM) and PBS was injected as the control. After 12 h post-injection, the tumor was irradiated with an 808 nm laser (1.25 W/cm^2) for 10 min. The thermal imaging of mice was carried out using an infrared thermal camera (FLIR) during the process of irradiation. After all the treatment, the weight and tumor volumes were recorded every two days. Equation: volume = length×width^2/2 was used to calculate the volume of tumors. All of the mice were sacrificed after 12 days of treatment. The tumors were isolated to photograph and their weights were recorded. The major organs (heart, liver, spleen, lungs, and kidneys) and tumors were fixed by 4% formalin solution for further histopathology analysis.

Supporting Figures

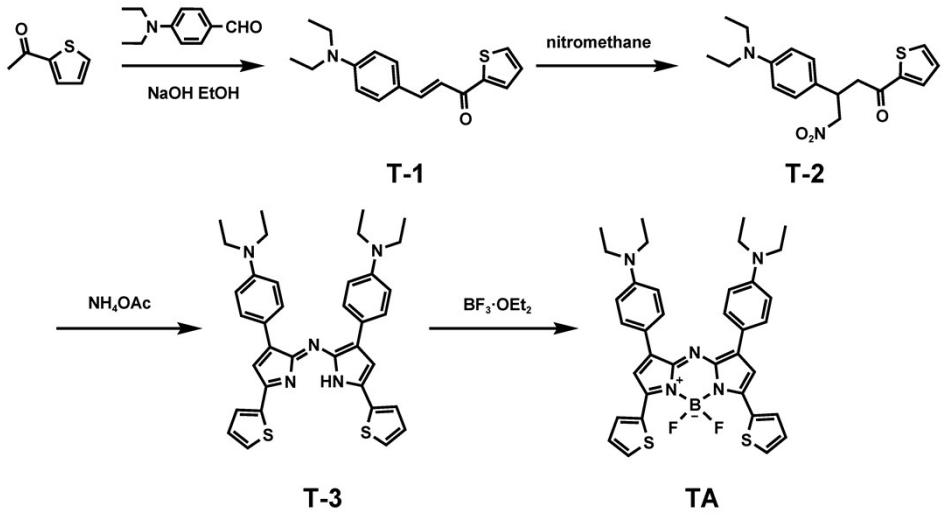

Figure S1. Synthetic route for TA.

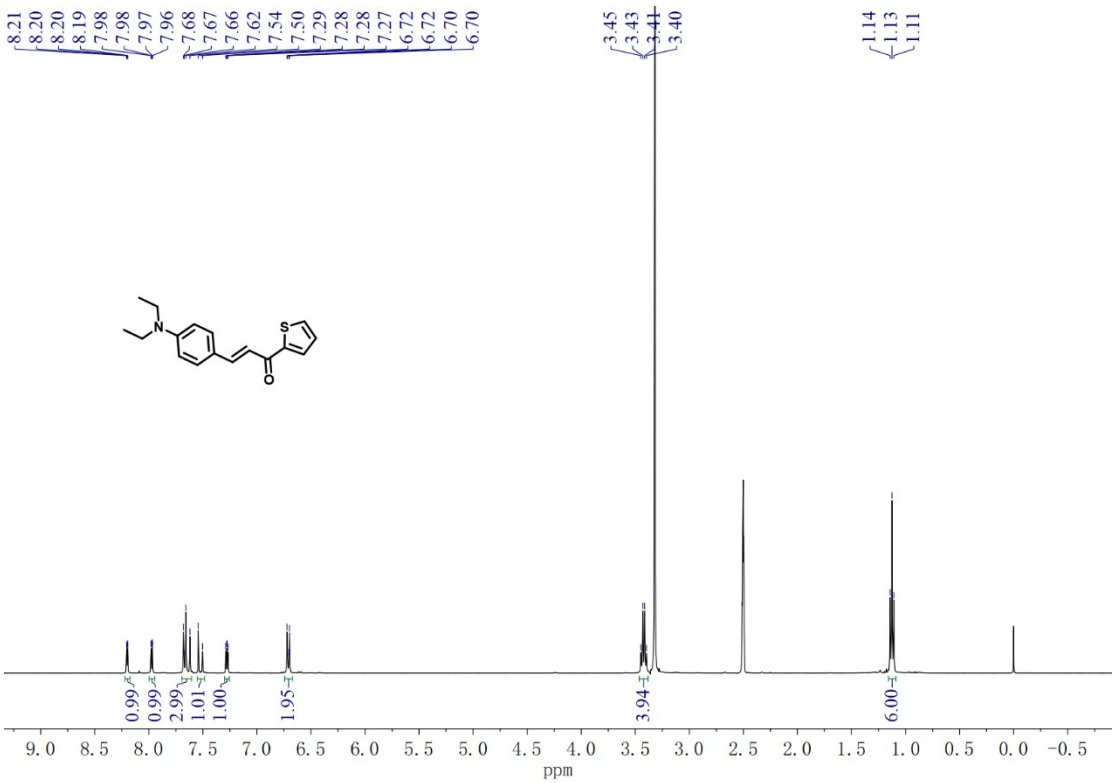

Figure S2. [1]H-NMR spectrum of T-1.

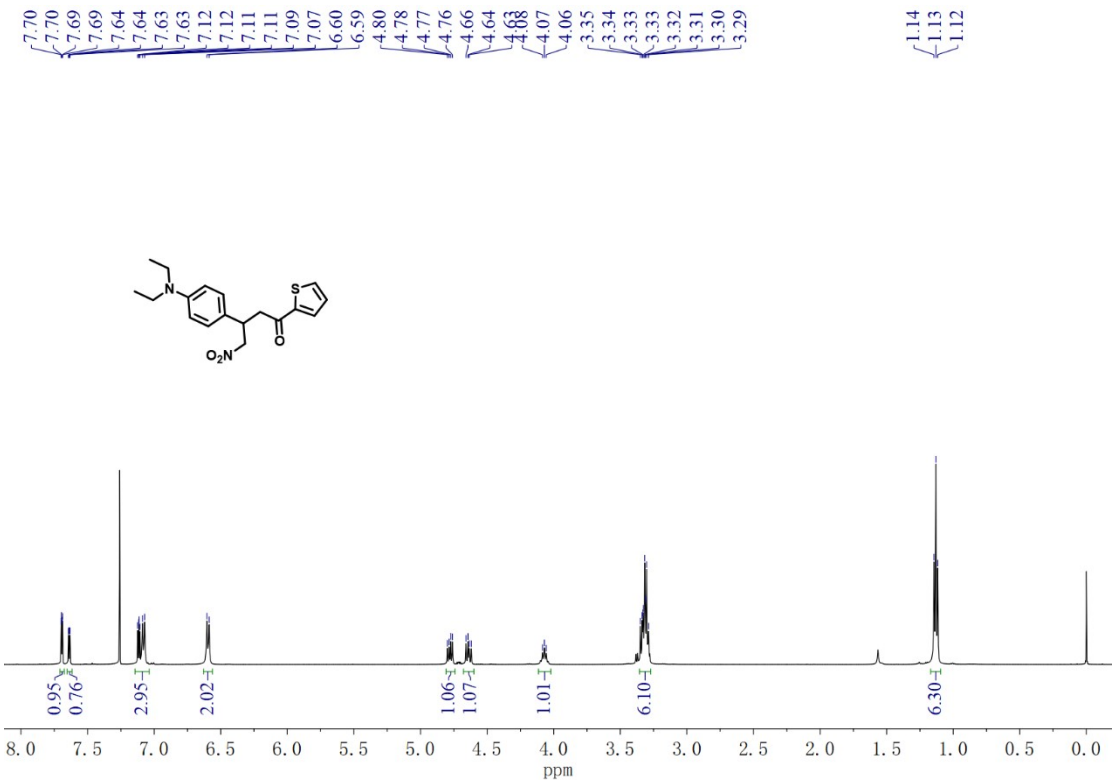

Figure S3. [1]H-NMR spectrum of T-2.

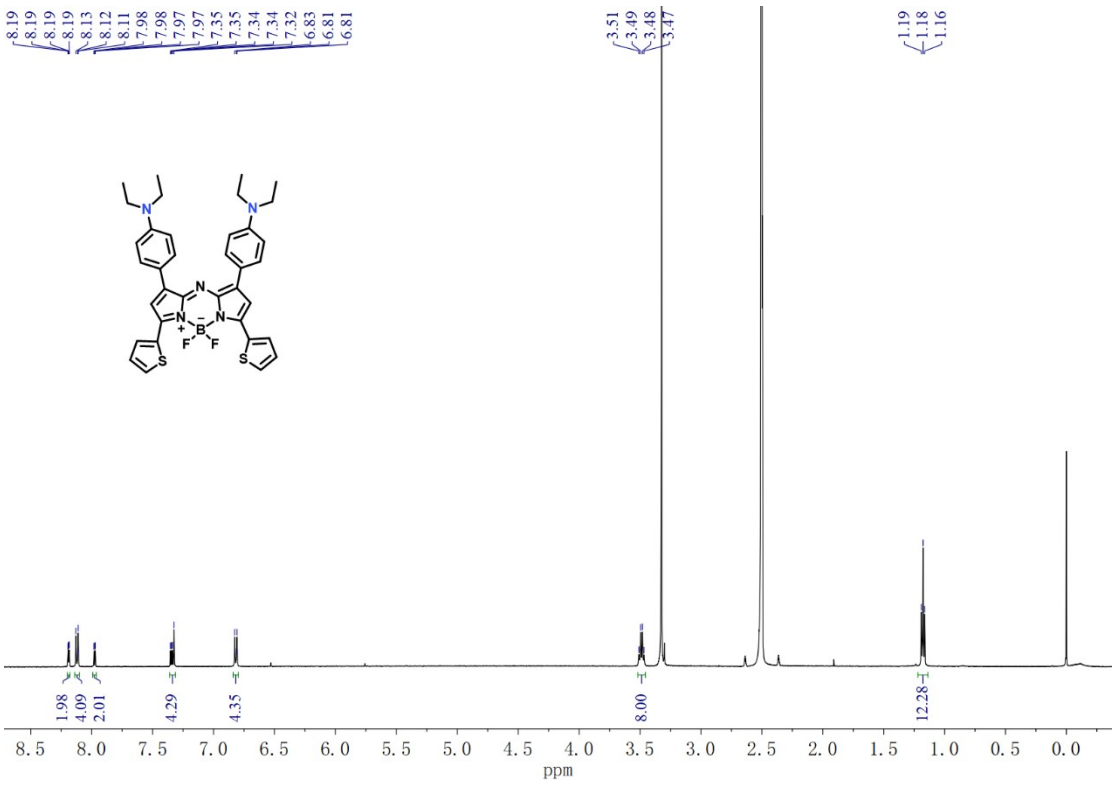

Figure S4. [1]H-NMR spectrum of TA.

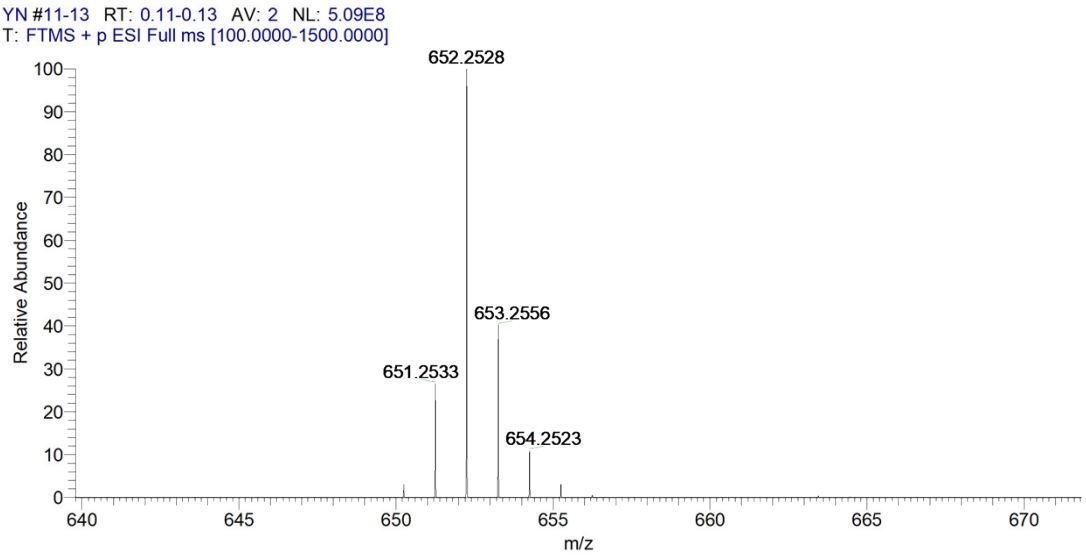

Figure S5. HR-MS spectrum of TA.

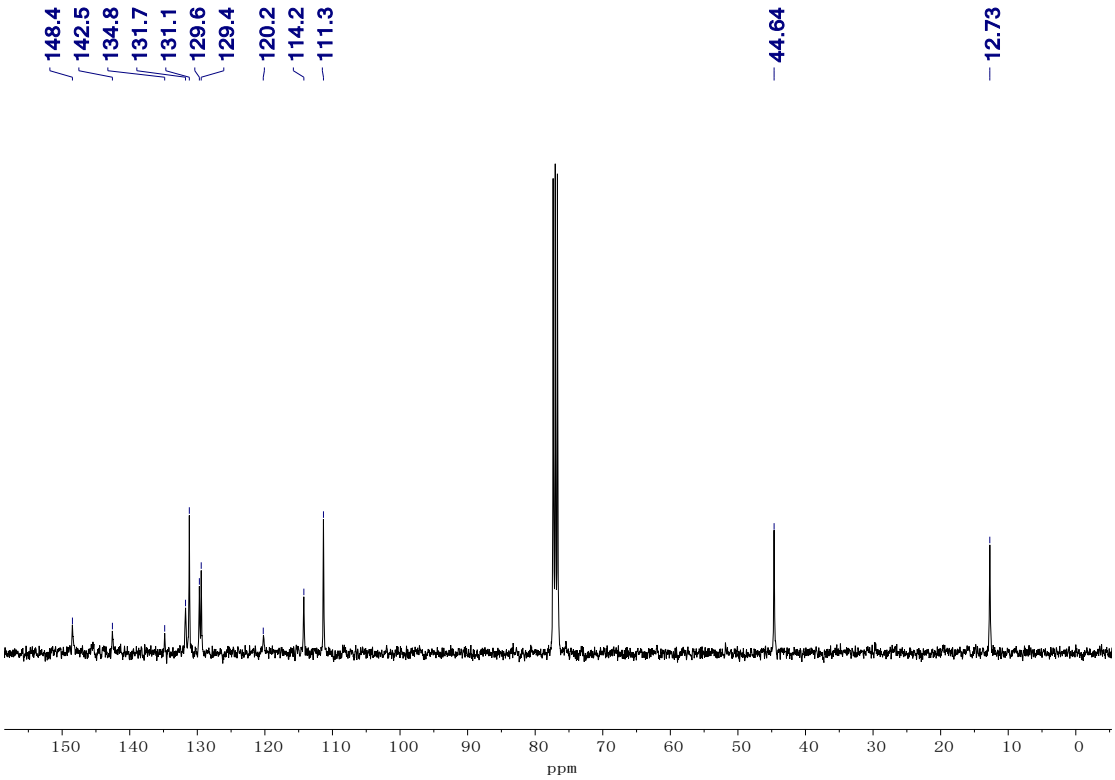

Figure S6. ^{13}C-NMR spectrum of TA.

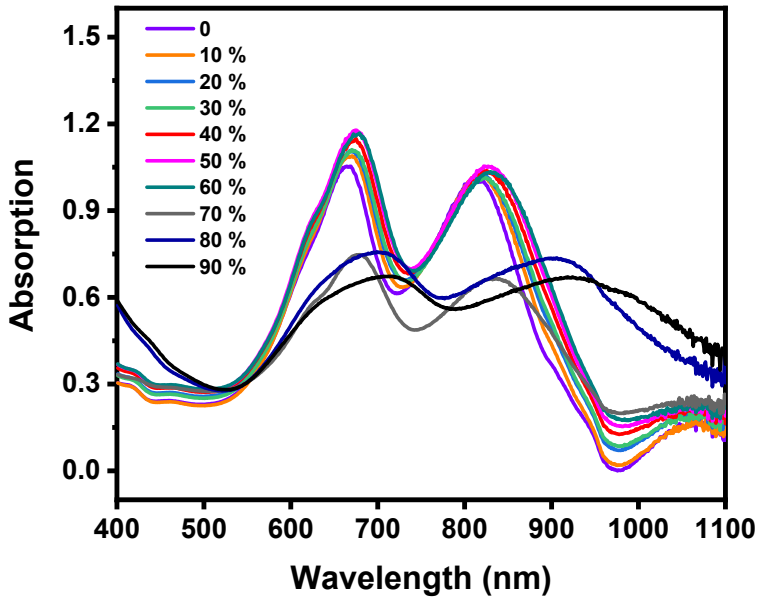

Figure S7. UV-vis absorption spectra of TA (20 μM) in THF-water binary solvent with varied water volumetric faction.

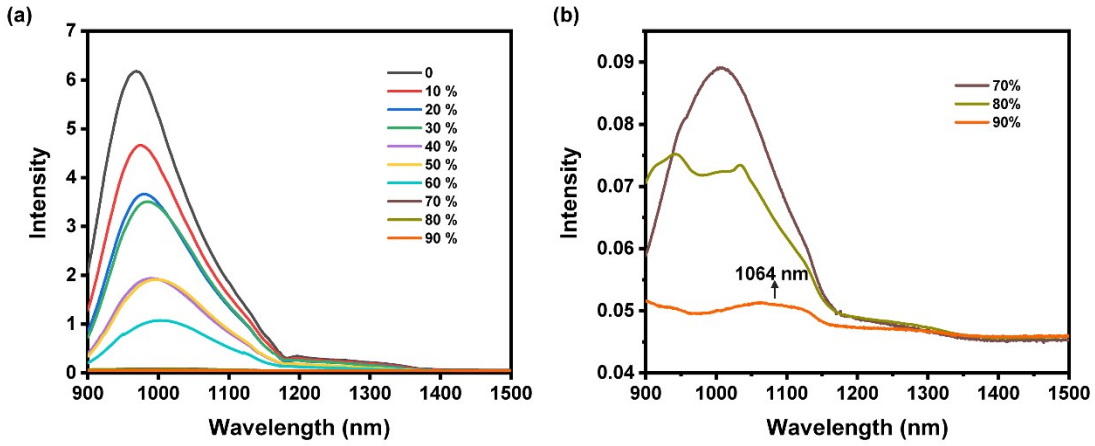

Figure S8. (a) Fluorescence spectra of TA (20 μM) in THF-water binary solvent with varied water volumetric faction. (b) Fluorescence spectra of TA (20 μM) in THF-water binary solvents with 70%-90% water volumetric fractions.

Table S1. Optimization study, the ratio between TA and polymer was varied to obtain the J-aggregates.

TA (mg)	Polymer (mg)	Maximum Emission (nm)	Fluorescence Intensity
0.2	10	975	0.562
0.5	10	1000	0.492
1	10	1020	0.238
1.5	10	1072	0.051

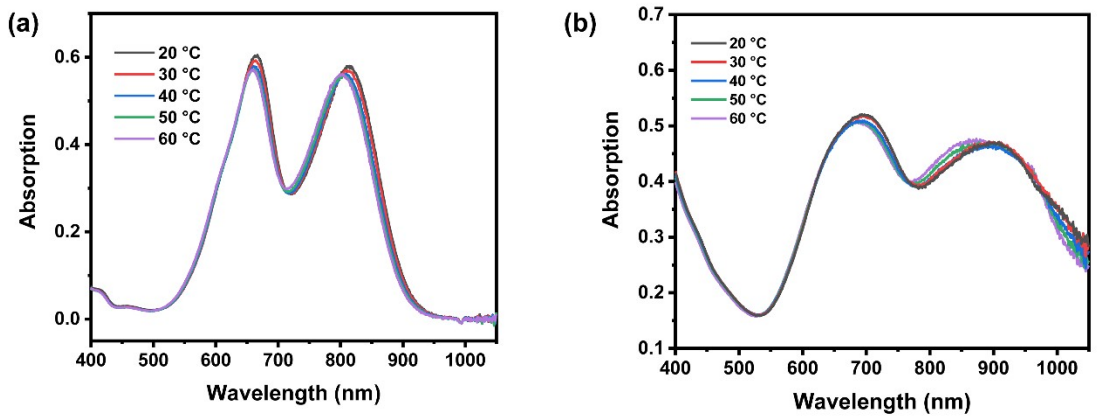

Figure S9. (a) Temperature-dependent absorption spectra of TA in THF. (b) Temperature-dependent absorption spectra of TA in THF/H_2O binary solution (f_w = 80%).

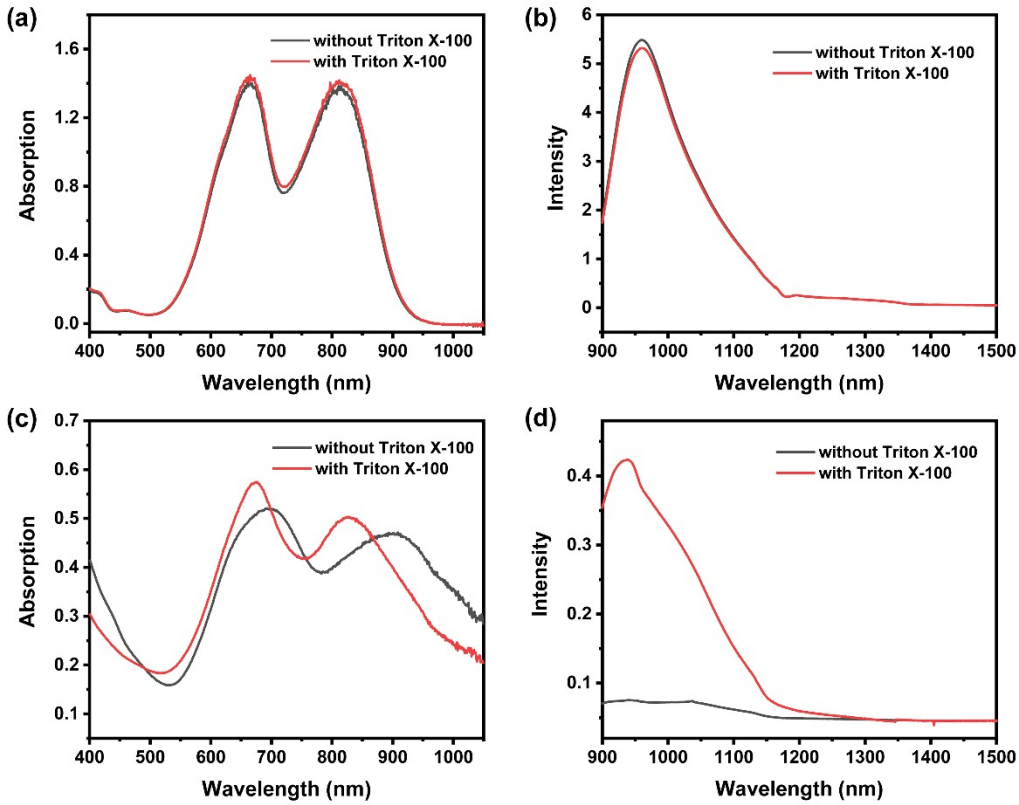

Figure S10. (a) Absorption spectra of TA in THF with/without Triton X-100. (b) Fluorescence spectra of TA in THF with/without Triton X-100. (c) Absorption spectra of TA in THF/H_2O binary solvent (f_w=80%) with/without Triton X-100. (d) Fluorescence spectra of TA in TFH/H_2O binary solvent (f_w=80%) with/without Triton X-100.

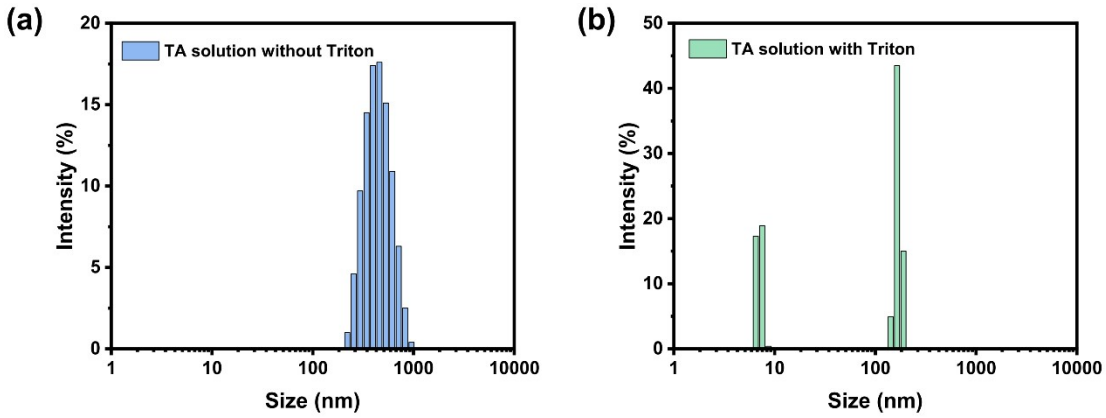

Figure S11. DLS size of TA in THF/H_2O (f_w = 80%) (a) without and (b) with the addition of Triton.

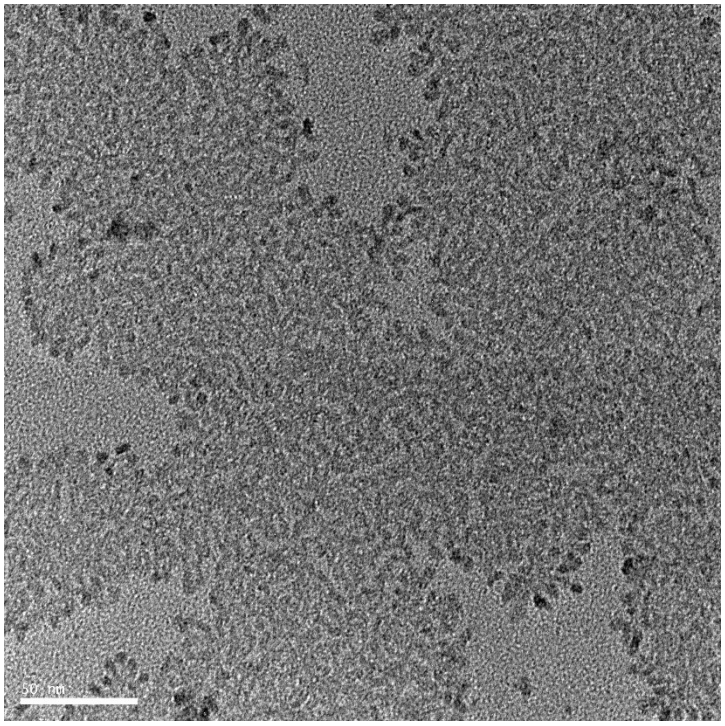

Figure S12. TEM image of TA aggregates.

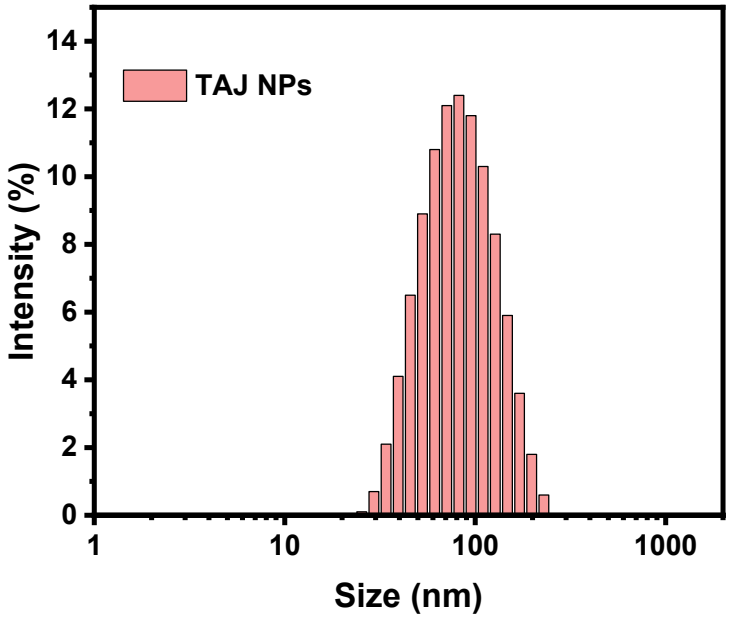

Figure S13. Dynamic light scattering (DLS) analysis of the TAJ NPs.

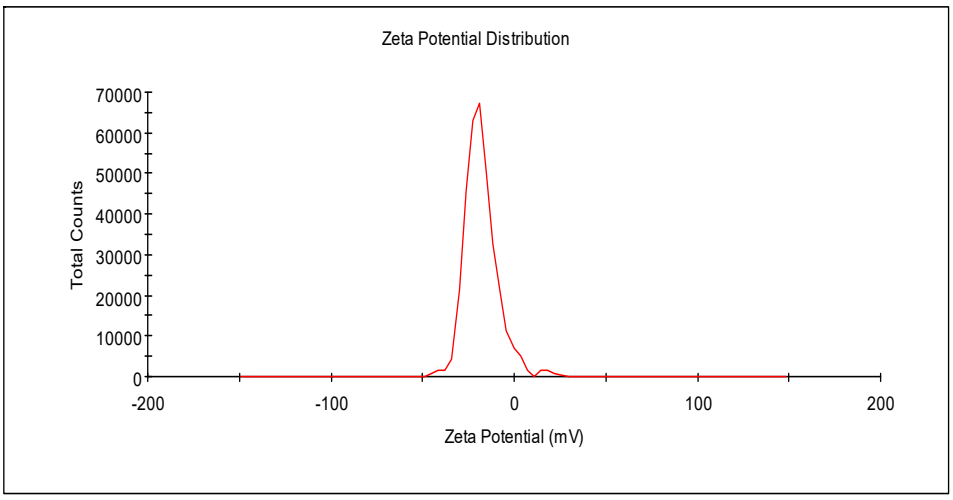

Figure S14. Zeta potential of the TAJ NPs in water.

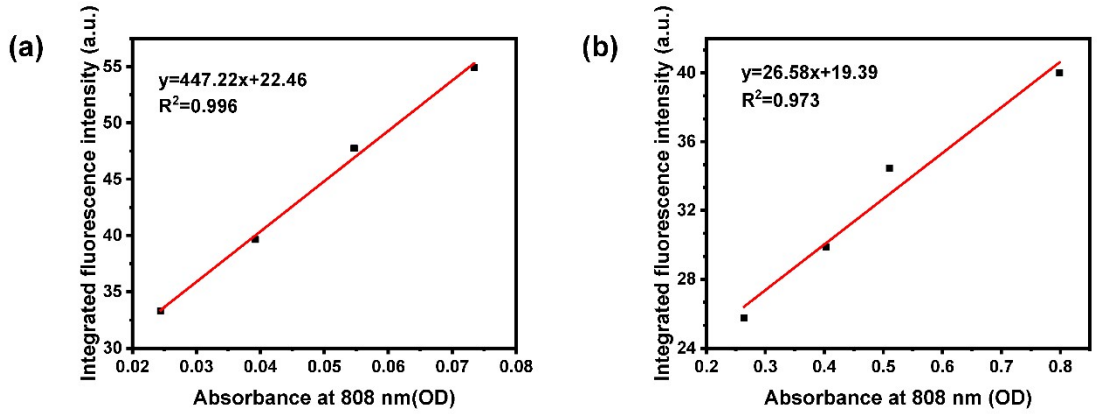

Figure S15. QY testing of TAJ NPs in PBS buffer. Data in NIR-II (1000-1500 nm) fluorescence quantum yield calculation. (a) Plot of integrated NIR-II fluorescence intensity vs the absorbance at 808 nm of Flav7 (QY = 0.53% in dichloroethane). (b) Plot of integrated NIR-II fluorescence intensity vs the absorbance at 808 nm of TAJ NPs in PBS buffer.

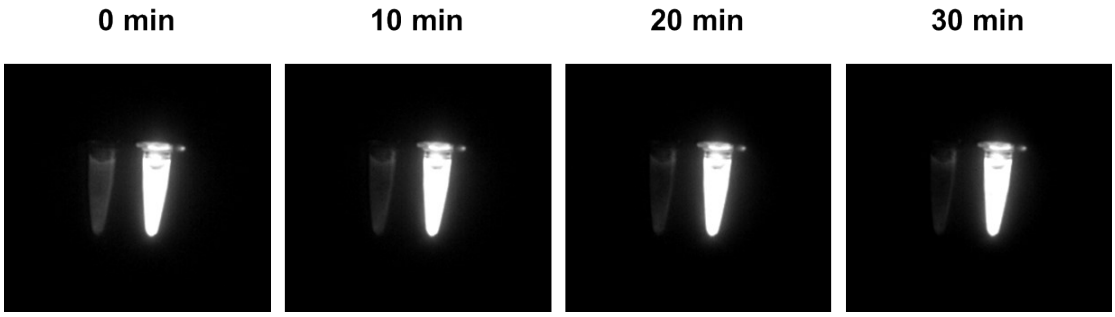

Figure S16. Brightness comparison of ICG (50 μM) and TAJ NPs (50 μM) after irradiation with 808 nm laser for different period of time (1100 LP).

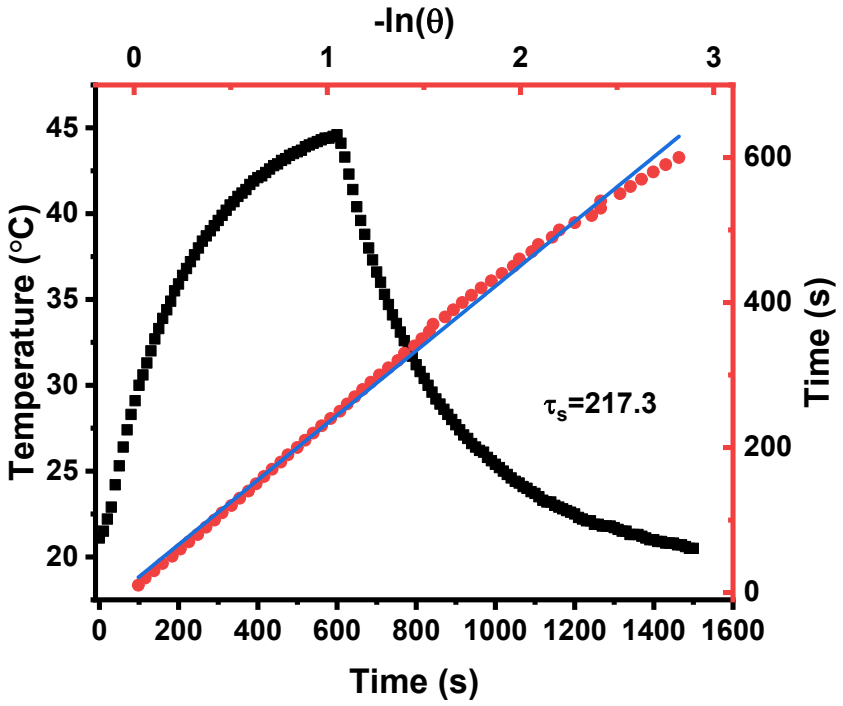

Figure S17. The photothermal response of TAJ NPs for 600 s with an 808 nm laser irradiation (1.25 W/cm^2) and then the laser was shut off and the corresponding blue line show linear time data versus -ln(θ) obtained from the cooling period.

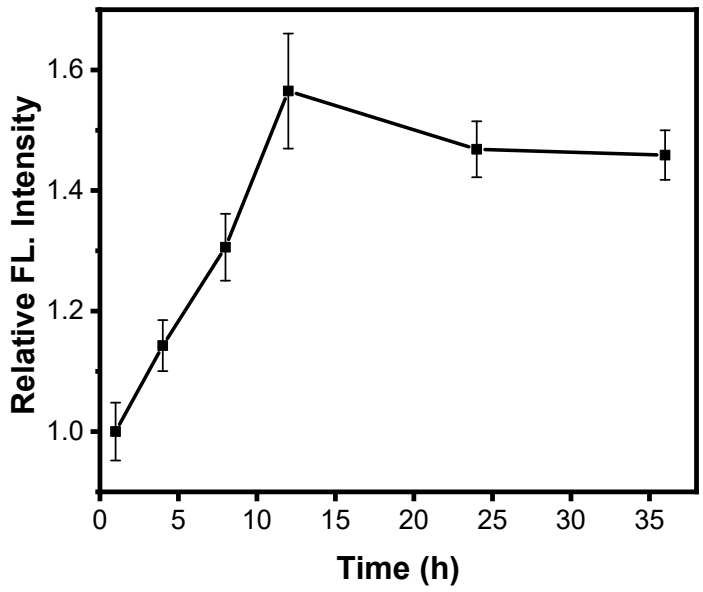

Figure S18. Semi-quantitative analysis of NIR-II fluorescence intensity of the tumor region using Image J software (n=3, mean ± SD).

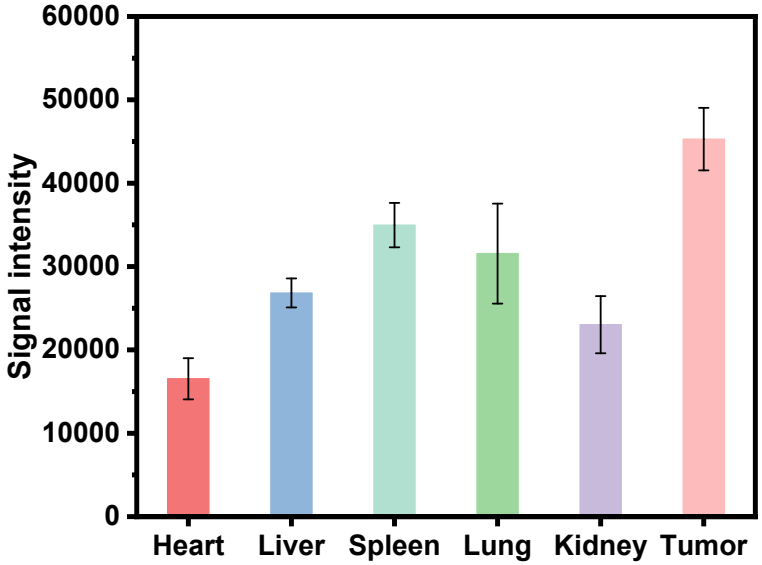

Figure S19. NIR-II fluorescence intensity of major organs and tumors 36 h post-injection (n=3, mean ± SD).

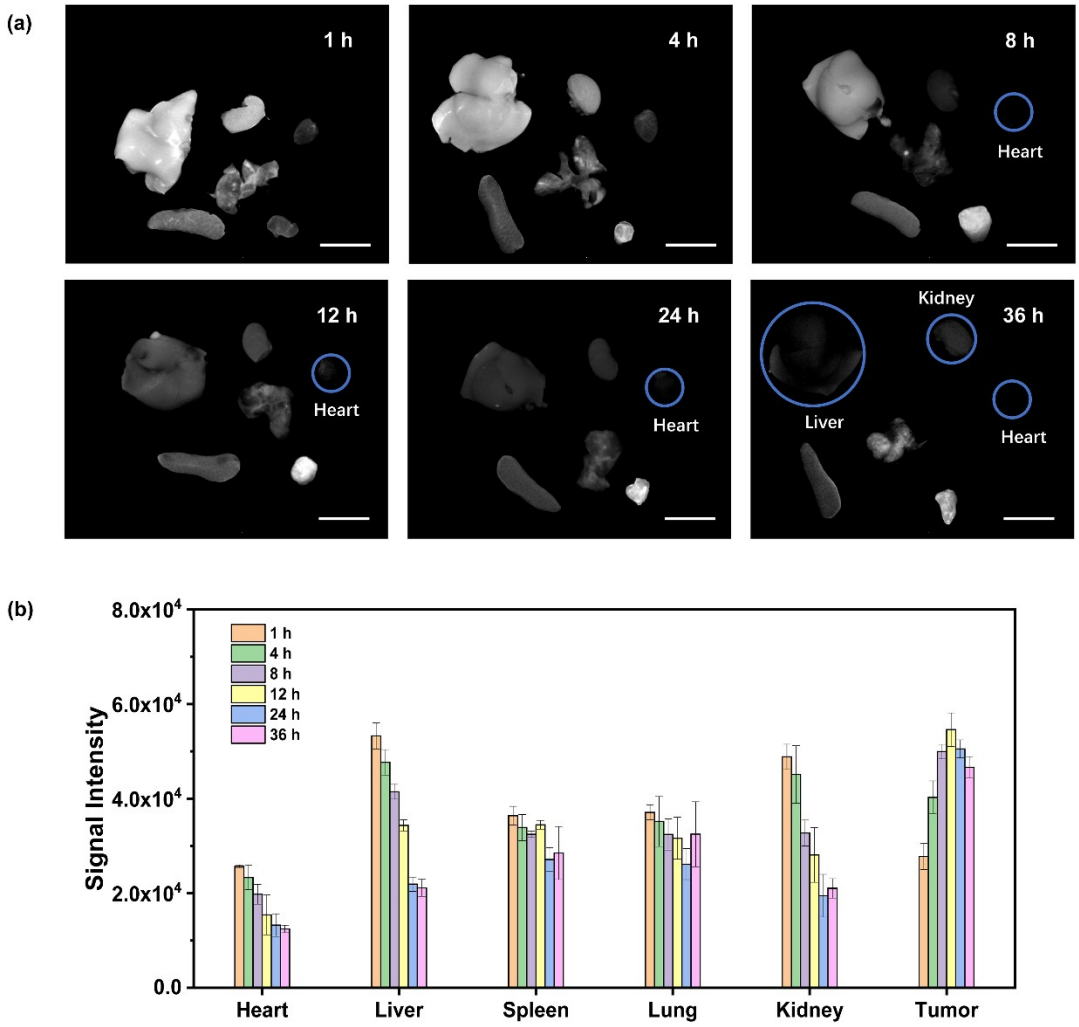

Figure S20. (a) Representative NIR-II fluorescence images of major organs and tumors after different time of post-injection (1200 LP, scale bar: 1 cm). (b) NIR-II fluorescence intensity of the major organs and tumors after different time of post-injection (n=3, mean ± SD).

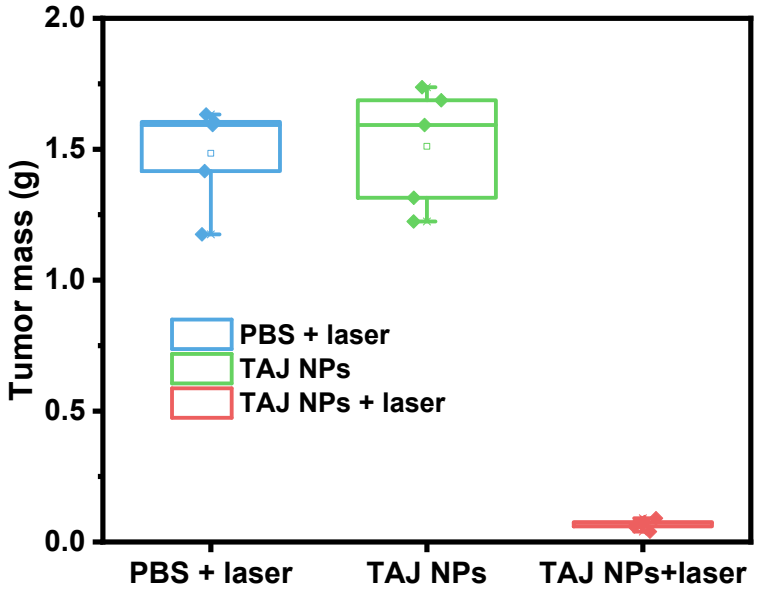

Figure S21. The tumor mass variation during 12-day treatment (n=5).

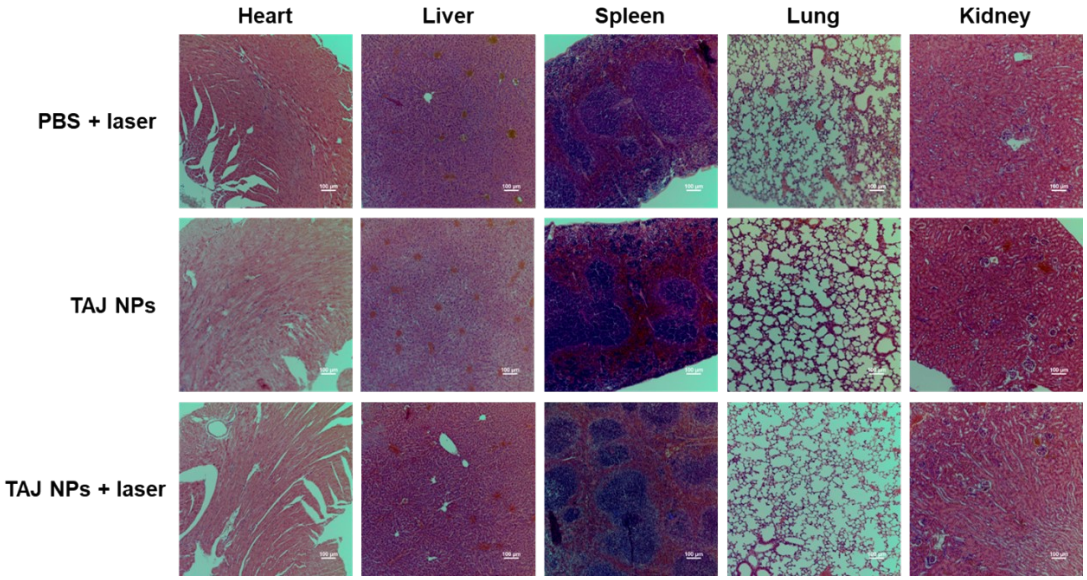

Figure S22. H&E staining of major organs of mice after 12 days of treatment. Scale bar: 100 μm

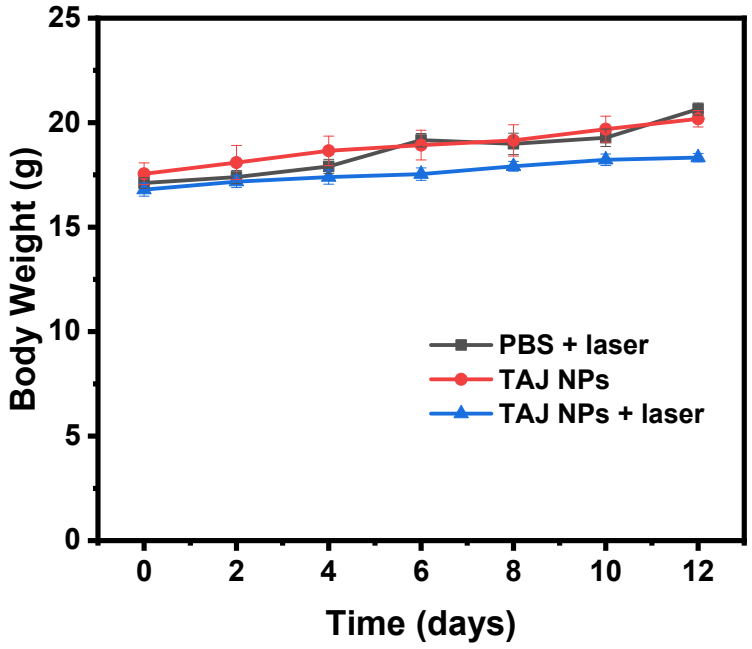

Figure S23. The weight variation in mice during treatment (n=5, mean ± SD).